International Atomic Energy Agency

INDC(CSR)-5/GI
INT(83)-7

INDC INTERNATIONAL NUCLEAR DATA COMMITTEE

γ-ray Production Cross Sections and γ-ray Multiplicities from Fe and Ni Bombarded with 14.6 MeV Neutrons

S. Hlavac and P. Oblozinsky

November 1983

IAEA NUCLEAR DATA SECTION, WAGRAMERSTRASSE 5, A-1400 VIENNA

Reproduced by the IAEA in Austria
November 1983
83-06520

INDC(CSR)-5/GI
INT(83)-7

γ-ray Production Cross Sections and γ-ray Multiplicities from Fe and Ni Bombarded with 14.6 MeV Neutrons

S. Hlavac and P. Oblozinsky

The data from this work have been compiled under the accession-number EXFOR-30801

November 1983

γ ray production cross sections and γ ray multiplicities from Fe and Ni bombarded with 14.6 MeV neutrons

S. Hlaváč and P. Obložinský

Institute of Physics, Electro-Physical Research Centre of the Slovak Academy of Sciences, 842 28 Bratislava, Czechoslovakia

Natural Fe, Ni and enriched ^{58}Ni were bombarded with 14.6 MeV neutrons to observe simultaneously Ge(Li), NaI(Tl) and neutron tof singles as well as coincidence spectra. Reported are 90-deg differential γ ray production cross sections in discrete as well as continuous spectral energy regions and average γ ray multiplicities related to several discrete transitions as well as to various energies of emitted neutrons.

Work partly performed under IAEA Co-operative Research Programme on the "Measurement and Analysis of 14 MeV Neutron Nuclear Data for Fission and Fusion Reactor Technology"

1. Introduction

Gamma ray production cross sections and γ ray spectra at 14 MeV incident neutron energy are important for calculations of shielding as well as nuclear heating in fusion and fission reactors (1). Such data are also of interest in studies concerning with physical concepts of γ ray emission (2). More detailed information, which is rather scarce here, can be obtained by measuring gated rather than singles spectra only. This piece of data can usually be presented in transparent way in terms of average γ ray multiplicities.

Here, we report experimental results obtained for Fe, Ni and ^{58}Ni. First, we briefly describe our experimental system and procedures, afterwards we present measured data.

2. Experimental procedures

We used a multidetector setup developed for combined spectrometry of continuous γ rays with discrete γ rays and neutrons at 14.6 MeV incident neutron energy. Detailed description of the system and experimental procedures is published elsewhere (3), here we give the most important points only.

Experimental arrangement is shown in fig.1. Neutrons are produced by 120 keV/100 μA separated D^+ beam bombarding a water cooled titanium-tritium target. Neutrons are collimated both by time correlated associated particles and by a massive collimator. The latter provides for effective shielding of 70 cm^3 Ge(Li), Ø16 cm x 10 cm NaI(Tl) and Ø12 cm x 4 cm NE 213 neutron tof spectrometer. Stilbene detector served as a neutron monitor.

The NaI(Tl) was surrounded by a lead shield to suppress background and by a lead collimator with Ø11 cm apperture to suppress Compton continuum in the detector response. The distance between the front face of the NaI(Tl) and the centre of the sample was 30 cm to allow for a time-of-flight based discrimination of neutrons.

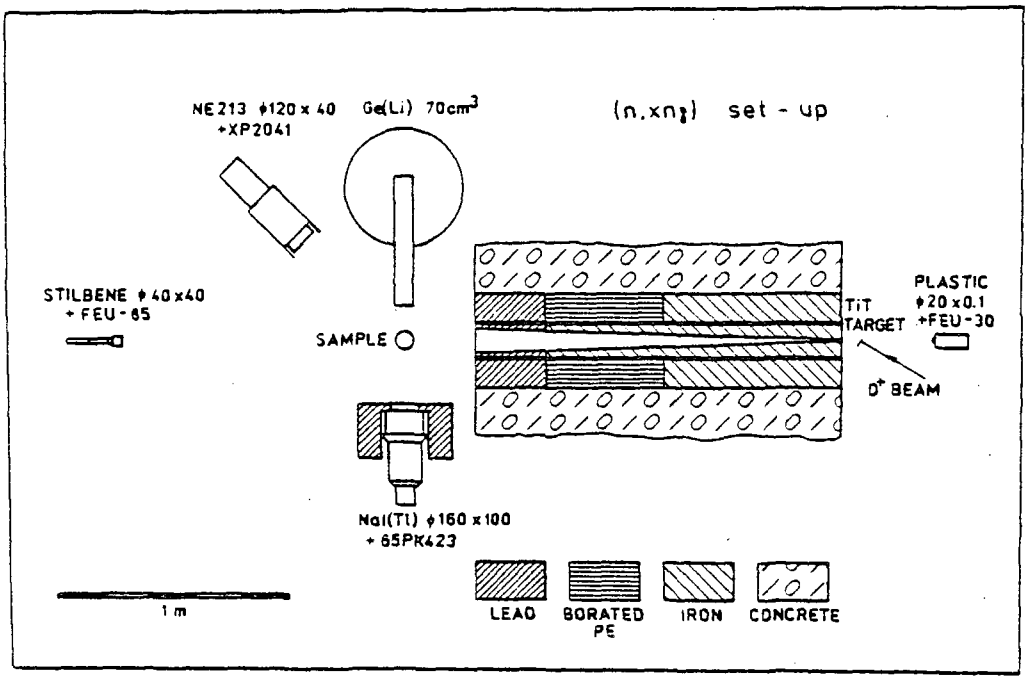

Fig. 1. Experimental arrangement.

Flight path for the NE 213 neutron tof spectrometer was 60 cm. Pulse shape discrimination was applied to distinguish between neutrons and γ rays.

Neutron fluence was measured in two ways. First, we used the associated α particle detector with corrections for actual solid angles and for the figure of merit of neutron collimation. The latter was determined experimentally. The second method was based on the absolutely calibrated stilbene monitor corrected for selfabsorption in the sample.

Discrete γ ray cross sections were obtained in a standard way from singles Ge(Li) spectra. To get continuous γ ray spectrum (for Fe sample only) we measured a twoparametric spectrum energy x time of the NaI(Tl) detector. Events due to neutrons registered in the detector as well as due to time uncorrelated background events were carefully subtracted and the resulting raw spectrum was unfolded.

Average γ ray multiplicities were obtained by comparing Ge(Li) spectrum measured in coincidence with the NaI(Tl) to the Ge(Li) singles spectrum. Similarly, average γ ray multiplicities for cascades following emission of neutrons

were obtained from the ratio of neutron tof spectrum measured in coincidence with the NaI(Tl) to the tof singles spectrum.

As samples we used natural Fe (232 g in a form of hollow cylinder Ø8/Ø7.7x8 cm^3 and 189 g in a planar form 8x10x0.3 cm^3), natural Ni (150 g in a planar form 8x8x0.3 cm^3) and ^{58}Ni (enriched to 99.5%, 100 g in a cylinder form). Corrections due to large volume of the samples were calculated by the Monte Carlo method. They varied from a couple of percents up to nearly 20%.

3. Results

3.1. Iron

Production cross sections for discrete γ rays measured at 90-deg towards the incident neutron beam are summarized in tab.1. We report 14 cross sections, of which 7 refer to ^{56}Fe transitions and 7 to ^{55}Fe transitions. The errors

Tab.1. 90-deg production cross sections of discrete γ rays from Fe+n.

E_γ (MeV)	Reaction	Transition	$\sigma_{rel}(90°)$	$\frac{d\sigma}{d\omega}(90°)$ (mb/sr)
Fe^{55} 412	(n,2nγ)	$1/2^- \rightarrow 3/2^-$	0.052(4)	2.04(29)
478	(n,2nγ)	$7/2^-_2 \rightarrow 5/2^-$	0.057(5)	2.24(34)
803	(n,2nγ)	$9/2^-_1 \rightarrow 7/2^-_2$	0.017(2)	0.67(11)
Fe^{56} 847	(n,n'γ)	$2^+_1 \rightarrow 0^+$	1.0	39.2(4.8)
931	(n,2nγ)	$5/2^- \rightarrow 3/2^-$	0.18(1)	7.06(94)
Fe^{56} 1038	(n,n'γ)	$4^+_2 \rightarrow 4^+_1$	0.098(6)	3.84(53)
1238	(n,n'γ)	$4^+_1 \rightarrow 2^+_1$	0.50(3)	19.6(2.7)
1303	(n,n'γ)	$6^+_1 \rightarrow 4^+_1$	0.11(1)	4.32(66)
1317	(n,2nγ)	$7/2^-_1 \rightarrow 3/2^-$	0.08(1)	0.31(5)
1369	(n,2nγ)	$9/2^-_2 \rightarrow 5/2^-$	0.012(3)	0.47(13)
1409	(n,2nγ)	$7/2^-_2 \rightarrow 3/2^-$	0.059(6)	2.31(37)
1671	(n,n'γ)	$6^+_2 \rightarrow 4^+_1$	0.061(6)	2.39(37)
1811	(n,n'γ)	$2^+_2 \rightarrow 2^+_1$	0.082(8)	3.32(50)
2113	(n,n'γ)	$2^+_3 \rightarrow 2^+_1$	0.026(5)	1.02(23)

Fe^{56} (N, N') Fe^{55}
Fe^{57} (N, 2N) Fe^{56}

hereafter given in brackets and refering to the last digits of measured quantities, include all essential contributions, see tab.2. Angle integrated production cross sections for the strongest 847 keV transition ($2_1^+ \rightarrow 0^+$ in ^{56}Fe) inferred from our 90-deg value and the angular distribution of ref.(4) is 560±70 mb.

Tab. 2. Table of errors of the discrete γ ray cross sections.

Source of error	Typical value (%)
No. of atoms in the sample	0.15
Neutron flux	4
Area of full energy peak (FEP)	0.5 - 10
Efficiency in FEP	5
Corrections	3
TOTAL	7 - 12

Continuous γ ray spectrum measured at 90-deg towards the incident neutrons is given in tab.3 and fig.2. The errors do not include a contribution due to the unfolding procedure. 90-deg total γ ray yield (above 0.2 MeV) is 256(16) mb/sr.

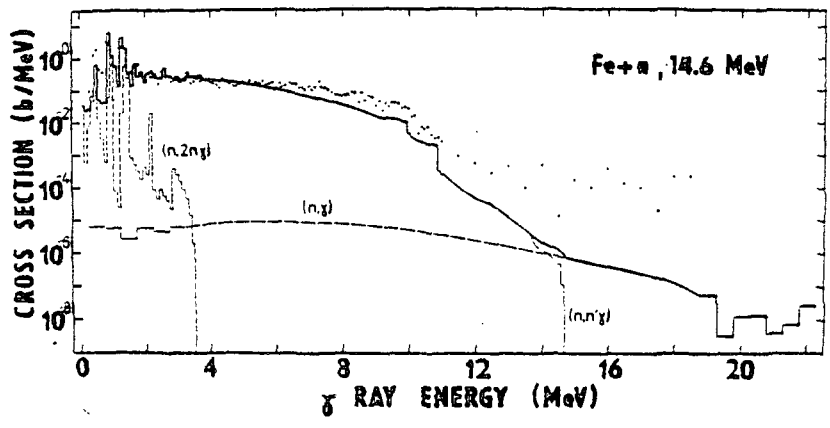

Fig.2. Spectrum of γ rays from Fe+n. Experimental values, see points, are 90-deg data multiplied by a factor of 4π. Histograms refer to spectra calculated in the frame of the statistical model for ^{56}Fe+n with the code STAPRE (for more details see ref. (5)).

Tab.3. 90-deg production cross sections of continuous γ rays from Fe+n. Energy step is 0.1 MeV up to 11 MeV and 0.5 MeV above 11 MeV.

E_γ (MeV)	$d^2\sigma/dEd\omega$ (b/MeV.sr)	E_γ (MeV)	$d^2\sigma/dEd\omega$ (b/MeV.sr)	E_γ (MeV)	$d^2\sigma/dEd\omega$ (b/MeV.sr)	E_γ (MeV)	$d^2\sigma/dEd\omega$ (b/MeV.sr)
0.2	8.85(63)-2	3.3	2.18(16)-2	6.4	1.37(11)-2	9.5	3.14(26)-3
0.3	8.22(58)-2	3.4	1.31(10)-2	6.5	1.17(9)-2	9.6	3.15(25)-3
0.4	1.05(8)-1	3.5	1.56(12)-2	6.6	1.27(10)-2	9.7	2.86(24)-3
0.5	1.40(10)-1	3.6	2.16(16)-2	6.7	9.90(72)-3	9.8	2.11(19)-3
0.6	3.58(25)-2	3.7	1.50(12)-2	6.8	9.68(71)-3	9.9	2.34(20)-3
0.7	2.91(21)-2	3.8	1.91(15)-2	6.9	7.80(57)-3	10.0	2.07(19)-3
0.8	2.69(19)-1	3.9	1.59(12)-2	7.0	1.06(8)-2	10.1	1.16(11)-3
0.9	2.36(17)-1	4.0	1.36(11)-2	7.1	8.31(61)-3	10.2	1.28(13)-3
1.0	5.03(36)-2	4.1	1.29(10)-2	7.2	1.02(8)-2	10.3	3.49(41)-4
1.1	4.43(31)-2	4.2	1.13(9)-2	7.3	8.45(62)-3	10.4	5.67(65)-4
1.2	1.65(12)-1	4.3	9.34(67)-3	7.4	1.05(8)-2	10.5	4.73(57)-4
1.3	1.71(12)-1	4.4	1.80(14)-2	7.5	9.01(66)-3	10.6	5.50(67)-4
1.4	4.46(32)-2	4.5	1.33(10)-2	7.6	8.67(64)-3	10.7	3.28(45)-4
1.5	2.53(18)-2	4.6	1.35(11)-2	7.7	6.89(51)-3	10.8	2.43(35)-4
1.6	3.28(23)-2	4.7	1.04(8)-2	7.8	5.49(41)-3	10.9	2.68(41)-4
1.7	4.28(30)-2	4.8	1.02(8)-2	7.9	5.59(42)-3	11.0	2.08(28)-4
1.8	4.93(35)-2	4.9	1.24(10)-2	8.0	5.14(38)-3	11.5	7.09(87)-5
1.9	2.76(20)-2	5.0	1.39(11)-2	8.1	5.51(41)-3	12.0	4.22(59)-5
2.0	2.08(15)-2	5.1	1.25(10)-2	8.2	5.72(43)-3	12.5	2.12(33)-5
2.1	2.71(19)-2	5.2	1.66(13)-2	8.3	6.82(51)-3	13.0	3.43(54)-5
2.2	2.02(14)-2	5.3	1.12(9)-2	8.4	6.58(50)-3	13.5	7.5(1.0)-6
2.3	2.11(15)-2	5.4	1.34(10)-2	8.5	3.39(26)-3	14.0	3.71(68)-5
2.4	1.22(9)-2	5.5	1.21(10)-2	8.6	6.24(47)-3	14.5	1.06(19)-6
2.5	3.17(23)-2	5.6	1.48(11)-2	8.7	3.73(29)-3	15.0	1.26(24)-5
2.6	2.56(19)-2	5.7	1.17(9)-2	8.8	4.86(37)-3	15.5	8.1(1.1)-6
2.7	2.24(16)-2	5.8	1.29(10)-2	8.9	4.64(36)-3	16.0	2.82(56)-5
2.8	1.45(11)-2	5.9	1.45(11)-2	9.0	2.63(21)-3	16.5	1.01(26)-5
2.9	1.59(12)-2	6.0	9.13(66)-3	9.1	3.61(28)-3	17.0	7.1(1.6)-6
3.0	1.56(12)-2	6.1	1.26(10)-2	9.2	1.81(15)-3	17.5	1.46(28)-6
3.1	1.37(11)-2	6.2	1.01(7)-2	9.3	3.01(24)-3	18.0	1.50(24)-5
3.2	1.74(13)-2	6.3	1.10(8)-2	9.4	2.38(20)-3	18.5	1.59(27)-5

Tab. 4. Average γ ray multiplicities including specific discrete transitions in ^{56}Fe from Fe+n.

Transition	E_γ (keV)	$\overline{M}$
$6^+ \rightarrow 4^+$	1303	7.1(1.9)
$4^+ \rightarrow 2^+$	1238	5.0(7)
$2^+ \rightarrow 0^+$	847	4.2(5)

Average γ ray multiplicities of cascades passing through a specific transition between low lying levels in ^{56}Fe are given in tab.4. The measurement was performed with the Ge(Li) located at 90-deg towards the beam and with the NaI(Tl) placed oppositely also at 90-deg. Since triple angular correlations are weak, as shown bellow, our data should be very close to angle integrated figures. Analysis of errors is given in the subsequent tab.5.

Tab. 5. Table of errors contributing to average γ multiplicities with a discrete transition.

Source of error	Typical value (%)
Area of FEP in singles spectrum	0.5
Area of FEP in coinc. spectrum	5 - 40
Total efficiency of NaI(Tl)	5
Corrections	5
TOTAL	9 - 41

Average γ ray multiplicities of cascades following after emission of a neutron with a given energy are summarized in tab.6. and fig.3. Uncertainty of the boundaries of the neutron energy bins starts from 8% at 1 MeV and increases to 29% at 12 MeV. Measurements were performed at 3 different positions of NE 213 versus fixed NaI(Tl). These positions were estimated by a simple model calculations to be most sensitive to reveal the triple angular correlation effect. The results show, however, that this effect is very weak.

Tab. 6. Average γ ray multiplicities of cascades which follow emission of a neutron with specific energy from Fe+n. The angles refer to positions of the NE 213 (polar angle, relative azimuthal angle).

E_n(MeV)	$\overline{M}$ (57°,180°)	$\overline{M}$ (120°,180°)	$\overline{M}$ (120°,90°)	Mean
1 - 2	2.2(5)	2.1(3)	2.4(2)	2.2(5)
2 - 3	3.2(6)	2.6(2)	3.0(3)	2.9(3)
3 - 4	3.2(6)	3.3(3)	2.7(3)	3.1(5)
4 - 5	3.2(9)	3.4(3)	3.4(4)	3.3(6)
5 - 6	3.2(9)	3.8(6)	2.7(6)	3.2(7)
6 - 7	3.0(9)	3.6(4)	4.3(7)	3.6(7)
7 - 8	3.1(5)	3.5(6)	3.4(9)	3.3(6)
8 - 10	2.4(4)	2.6(6)	2.5(5)	2.5(5)
10 - 12	2.2(5)	---	---	2.2(5)

Excitation energy after emission of a neutron as shown in the upper scale of fig. 3 refers to the dominating isotop ^{56}Fe (91.8% in natural Fe). At excitation energies above the neutron binding, the multiplicities bent down due to admixture of cascades from the (n,2nγ) channel into the (n,n'γ) one. This makes it possible to extract average radiative widths above neutron or proton binding energy (2).

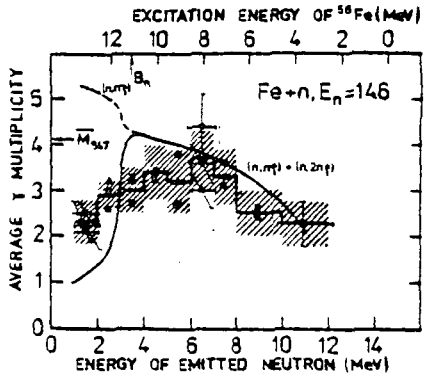

Fig. 3. Average γ ray multiplicity as a function of energy of emitted neutron from Fe+n. The curves are theoretical values calculated with modified code STAPRE (6).

3.2. Nickel

Production cross sections for discrete γ rays measured at 90-deg towards the neutron beam are given in tab. 7. The contributions to errors are the same as shown already in tab.2.

Tab. 7. 90-deg production cross sections of discrete γ rays from Ni+n.

E_γ(keV)	Reaction	Transition	$\frac{d\sigma}{d\omega}(90°)$(mb/sr)
230	^{60}Ni(n,pγ)	$3^+ \rightarrow 2^+$	0.61(6)
277	^{60}Ni(n,pγ)	$4^+ \rightarrow 5^+$	0.80(8)
321	^{58}Ni(n,pγ)	$5^+ \rightarrow 4^+$	1.27(10)
339	^{60}Ni(n,2nγ)	$5/2^- \rightarrow 3/2^-$	8.44(72)
366	^{58}Ni(n,pγ)	$3^+ \rightarrow 2^+$	1.28(9)
412	^{58}Ni(n,$\alpha\gamma$)	$1/2^- \rightarrow 3/2^-$	0.25(3)
433	^{58}Ni(n,pγ)	$4^+ \rightarrow 5^+$	1.43(12)
448	^{60}Ni(n,pγ)	$3^+ \rightarrow 2^+$	0.56(8)
465	^{58}Ni(n,n'pγ)	$11/2^- \rightarrow 9/2^-$	1.43(11)
478	^{58}Ni(n,$\alpha\gamma$)	$7/2^- \rightarrow 5/2^-$	0.90(8)
673	^{58}Ni(n,n'pγ)	$7/2^- \rightarrow 9/2^-$	0.53(6)
726	^{58}Ni(n,pγ)	$5^+ \rightarrow 4^+$	0.61(6)
745	^{58}Ni(n,n'γ)	$6 \rightarrow 5$	0.49(7)
762	^{58}Ni(n,n'γ)	$5 \rightarrow 4^+$	0.63(6)
769	^{58}Ni(n,2nγ)	$5/2^- \rightarrow 3/2^-$	0.56(6)
774	^{58}Ni(n,pγ)	$4^+ \rightarrow 3^+$	0.41(5)
803	^{58}Ni(n,$\alpha\gamma$)	$9/2^- \rightarrow 7/2^-$	0.70(7)
826	^{60}Ni(n,n'γ)	$2^+ \rightarrow 2^+$	6.05(47)
833	^{58}Ni(n,pγ)	$4^+ \rightarrow 4^+$	0.59(7)
878	^{60}Ni(n,2nγ)	$3/2^- \rightarrow 3/2^-$	1.83(16)
931	^{58}Ni(n,$\alpha\gamma$)	$5/2^- \rightarrow 3/2^-$	1.91(17)
961	^{58}Ni(n,n'γ)	$? \rightarrow 4^+$	0.81(8)
1005	^{58}Ni(n,n'γ)	$4^+ \rightarrow 2^+$	6.21(45)
1051	^{58}Ni(n,pγ)	$? \rightarrow 2^+$	1.67(16)
1160	^{58}Ni(n,n'γ)	$4^+ \rightarrow 4^+$	1.66(16)
1173	^{60}Ni(n,n'γ)	$4^+ \rightarrow 2^+$	19.3(1.2)
1189	^{60}Ni(n,2nγ)	$5/2^- \rightarrow 3/2^-$	2.15(32)
1223	^{58}Ni(n,npγ)	$9/2^- \rightarrow 7/2^-$	7.64(51)

Tab. 7. cont.

1317	^{58}Ni(n,$\alpha\gamma$)	$7/2^- \rightarrow 3/2^-$	0.95(9)
1321	^{58}Ni(n,n'γ)	$2^+ \rightarrow 2^+$	0.80(8)
1332	^{60}Ni(n,n'γ)	$2^+ \rightarrow 0^+$	40.6(3.6)
1378	^{58}Ni(n,n'pγ)	$3/2^- \rightarrow 7/2^-$	2.31(17)
1409	^{58}Ni(n,$\alpha\gamma$)	$7/2^- \rightarrow 3/2^-$	0.56(8)
1454	^{58}Ni(n,n'γ)	$2^+ \rightarrow 0^+$	15.9(1.2)
1689	^{58}Ni(n,n'pγ)	$11/2^- \rightarrow 7/2^-$	0.79(8)
1757	^{58}Ni(n,n'pγ)	$3/2^- \rightarrow 7/2^-$	0.72(8)
1919	^{58}Ni(n,n'pγ)	$5/2 \rightarrow 7/2^-$	0.64(8)

Average γ ray multiplicities of cascades passing through specific transition in ^{58,60}Ni and ^{57,58}Co are given in tab. 8. The measurement was performed with the Ge(Li) at 90-deg and the NaI(Tl) placed symetrically also at 90-deg towards the beam. The errors were analysed already in tab. 5.

Tab. 8. Average multiplicities from Ni+n including specific transition in ^{58,60}Ni and ^{57,58}Co.

E_γ(keV)	Reaction	Transition	$\overline{M}$
321	^{58}Ni(n,pγ)^{58}Co	$5^+ \rightarrow 4^+$	4.6(5)
1005	^{58}Ni(n,n'γ)^{58}Ni	$4^+ \rightarrow 2^+$	5.4(5)
1160	^{58}Ni(n,n'γ)^{58}Ni	$4^+ \rightarrow 4^+$	6.4(1.0)
1173	^{60}Ni(n,n'γ)^{60}Ni	$4^+ \rightarrow 2^+$	4.4(5)
1223	^{58}Ni(n,n'pγ)^{57}Co	$9/2^- \rightarrow 7/2^-$	1.5(8)
1332	^{60}Ni(n,n'γ)^{60}Ni	$2^+ \rightarrow 0^+$	3.9(4)
1454	^{58}Ni(n,n'γ)^{58}Ni	$2^+ \rightarrow 0^+$	4.8(4)

Average γ ray multiplicities connected with emitted neutrons from ^{58}Ni+n are given in tab. 9. and fig. 4. They were measured with the NE 213 at 60-deg and NaI(Tl) at 90-deg towards the neutron beam, the relative azimuthal angle being 180-deg. Residual excitation energy of ^{58}Ni is also shown in fig. 4. Above the proton binding energy the experimental multiplicities bent down due to admixture of (n,n'pγ) channel into the (n,n'γ) one.

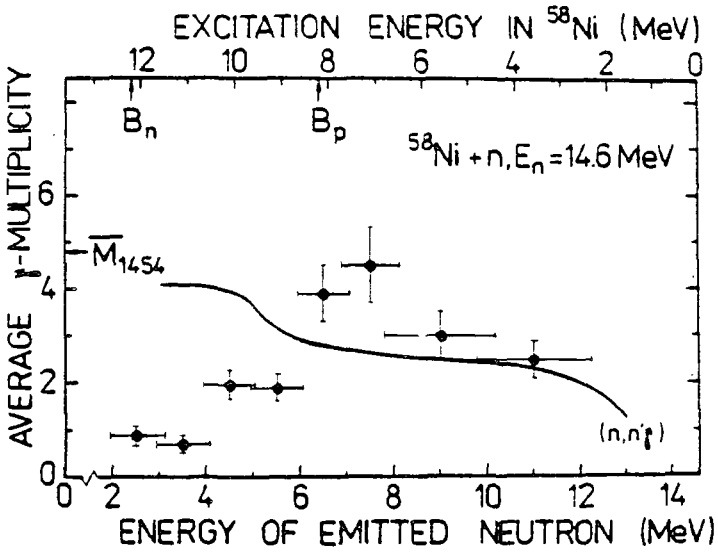

Fig. 4. Average γ ray multiplicities of cascades following emission of a neutron from ^{58}Ni+n. Experimental values are those of tab. 9 , full curve (7) is statistical model calculation for ^{58}Ni(n,n'γ).

Tab. 9. Average γ ray multiplicities of cascades after emission of a neutron from ^{58}Ni+n.

E_n (MeV)	$\overline{M}$
2 - 3	0.9(5)
3 - 4	0.7(5)
4 - 5	2.0(3)
5 - 6	1.9(3)
6 - 7	3.9(6)
7 - 8	4.5(8)
8 - 10	3.0(5)
10 - 12	2.5(4)

References

(1) N. Kocherov and J. J. Schmidt eds., IAEA Report INDC(NDS)-122/L, Vienna 1980

(2) S. Hlaváč, Thesis, Bratislava 1982, unpublished

(3) S. Hlaváč and P. Obložinský, Nucl. Instr. Meth. 206(1983)127

(4) A. P. Degtyarev, J. E. Kozyr and G. A. Prokopets, Ukr. Fiz. Zh. 22(1977)1463

(5) R. Antalík, S. Hlaváč and P. Obložinský, Report ZfK-459, (G. Musiol, W. Wagner, M. Josh eds.,Rossendorf 1981)p.153

(6) S. Hlaváč, P. Obložinský and R. Antalík, Bull. Acad. Sci. USSR, Phys. Ser. 46(1982)903

(7) S. Hlaváč, P. Obložinský, R. Antalík and J. Pivarč, in Neutron Induced Reactions, Proc. Europhysics Topical Conf. (P. Obložinský ed., Bratislava 1982) p.239